

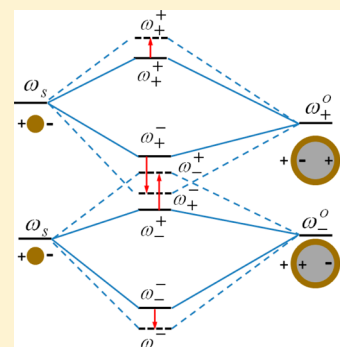
# Localized Hybrid Plasmon Modes Reversion in Gold–Silica–Gold Multilayer Nanoshells

Jun Qian, Yudong Li, Jing Chen, Jingjun Xu, and Qian Sun\*

MOE Key Laboratory of Weak Light Nonlinear Photonics, Tianjin Key Laboratory of Photonics Material and Technology, School of Physics, Nankai University, Tianjin 300071, China

## Supporting Information

**ABSTRACT:** The plasmon hybridization theory is widely used to study the plasmon response of metallic nanostructures. In this work, we study the plasmon hybridization picture of the gold–silica–gold multilayer nanoshells from the viewpoint of the optical extinction spectrum and the charge density distribution. We find that reducing the distance between the Au core and the Au shell causes the conversion from  $|\omega_{-}^{+}\rangle$  to  $|\omega_{+}^{-}\rangle$  modes of the high energy extinction peak. According to our opinion, it is because the increased plasmon interaction between the Au core and the Au shell induces the energy reversion of the  $|\omega_{+}^{+}\rangle$  and  $|\omega_{-}^{-}\rangle$  plasmon modes. The interesting contrary shift effect of the high energy extinction peaks with different dielectric constants of the middle silica shell and outer surrounding is well-explained by the  $|\omega_{+}^{-}\rangle$  modes. The energy reversion of hybrid plasmon modes we reported would give new insight into the plasmon hybridization theory. Moreover, our study could offer a modified way based on the charge interaction analysis, which is a necessary supplement to the plasmon hybridization theory, for studying plasmon responses in the optical spectrum of metal nanostructures.



## 1. INTRODUCTION

In recent years, dielectric metal core–shell nanostructures have generated great interest due to their unique electronic and optical properties that are dominated by the localized surface plasmon resonance (LSPR). In particular, the gold nanoshell has attracted significant attention because of its applications in biotechnology and biomedicine.<sup>1–3</sup> In Au nanoshells, the plasmon resonance can be tuned from visible to near-infrared “water window”, a transparent window for biological tissues, by increasing the ratio of the core size to shell thickness. Recently, the Au–silica–Au multilayer nanoshells have been fabricated and widely studied.<sup>4–13</sup> Compared with the Au nanoshell, the Au–silica–Au nanoshells can provide more tunable plasmon resonance while maintaining the small size as a result of the plasmon mode interaction between the inner Au sphere and the outer Au shell. Moreover, the tunable Fano resonances can be achieved in the symmetric<sup>14</sup> or unsymmetric Au–silica–Au nanoshells.<sup>15–17</sup>

The plasmon hybridization theory is widely used to study the plasmon response of metallic nanostructures.<sup>18–20</sup> In this theory, the plasmon response of the metallic nanostructures is explained by the interaction between the plasmons of metallic nanostructures in more elementary shapes. The Au nanoshells and multilayer shells are the representative examples for the theoretical investigation of plasmon hybridization. The plasmon resonance of a Au nanoshell can be considered as the interaction between the plasmons of a Au sphere and a dielectric cavity. The hybridization of the plasmons of the sphere and the cavity creates two new plasmon modes, i.e., the higher-energy antibonding mode  $|\omega_{+}\rangle$  and the lower-energy

bonding mode  $|\omega_{-}\rangle$ , corresponding to the antisymmetric and symmetric interactions between the sphere and the cavity modes, respectively. Furthermore, the plasmon resonance in a Au–silica–Au multilayer nanoshell<sup>5,8</sup> can be viewed as the interaction between the plasmon modes of the inner core sphere  $|\omega_s\rangle$  and the outer nanoshell bonding ( $|\omega_{+}^o\rangle$ ) and antibonding ( $|\omega_{-}^o\rangle$ ) modes. As shown in Figure 1b, the hybridization of the  $|\omega_s\rangle$  and  $|\omega_{-}^o\rangle$  modes gives rise to the two lower-energy  $|\omega_{-}^{-}\rangle$  and  $|\omega_{-}^o\rangle$  modes, and the hybridization of the  $|\omega_s\rangle$  and  $|\omega_{+}^o\rangle$  modes gives rise to the two higher-energy  $|\omega_{+}^{-}\rangle$  and  $|\omega_{+}^o\rangle$  modes. The higher-energy  $|\omega_{+}^{-}\rangle$  and  $|\omega_{+}^o\rangle$  modes are usually too weak to be observed in the optical spectrum. Recently, it is reported that the  $|\omega_{+}^{-}\rangle$  modes may occur in the optical spectrum by choosing an appropriate dielectric constant of the silica layer and geometrical dimensions of the inner core and outer shell in Au–silica–Au<sup>7</sup> or Au–silica–Ag<sup>21</sup> multilayer nanoshells.

In the previous study, the observed high energy and low energy peaks in the optical spectrum of Au–silica–Au multilayer nanoshells are always described by the  $|\omega_{+}^{-}\rangle$  mode and  $|\omega_{-}^{-}\rangle$  mode, respectively. However, in our study, we find that, with the decreasing of the distance between the Au core and the Au shell, the high energy peak in the optical spectrum can be converted from  $|\omega_{+}^{-}\rangle$  to  $|\omega_{-}^{-}\rangle$  modes. In our opinion, reducing the distance between the Au core and the Au shell increases the plasmon interaction between them and can lead

Received: January 21, 2014

Revised: March 23, 2014

Published: March 31, 2014

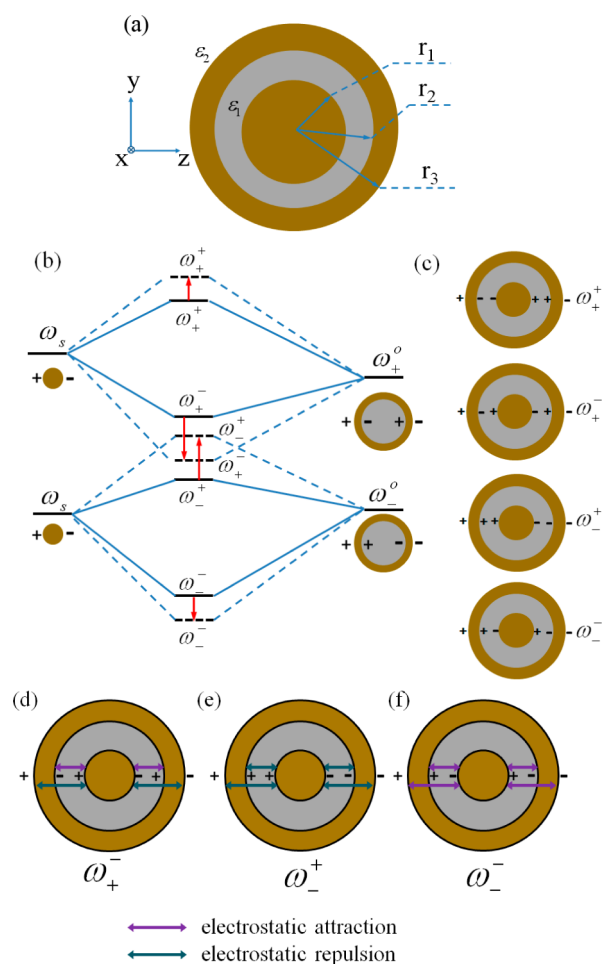


**Figure 1.** (a) Midsectional view of the Au–silica–Au multilayer nanoshells. (b) Schematic of energy diagram of the inner Au core and outer Au shell, representing plasmon hybridization. The dashed line indicates the coupling modes under enhanced interaction between the Au core and the Au shell. (c) Schematic of the charge distribution of the coupling modes in the Au–silica–Au multilayer nanoshells according to the plasmon hybridization. (d–f) Schematics of the charge interaction between the Au core and the Au shell in the  $\omega_+^-$ ,  $\omega_+^+$ , and  $\omega_-^-$  plasmon modes of Au–silica–Au multilayer nanoshells.

to the energy enhancement of the  $\omega_+^+$  mode and the energy reduction of the  $\omega_+^-$  mode, which results in the energy reversion of the  $\omega_+^-$  and  $\omega_+^+$  modes in the plasmon hybridization picture.

The shift of the high energy extinction peaks with the increasing in the Au core radius in Au–silica–Au nanoshells is a puzzling question. Both of the blue shifts<sup>5</sup> and the red shifts<sup>6</sup> of the high energy peaks have been found by different research groups. Recently, Zhu et al.<sup>7</sup> demonstrated that the high energy extinction peaks blue shift when the dielectric constant of the middle silica layer is larger than that of the embedding medium, whereas the high energy extinction peaks red shift when the dielectric constant of the middle silica layer is smaller than that of the embedding medium. It is difficult to explain this contrary shift effect by the  $\omega_+^+$  mode in plasmon hybridization theory. In our study, the contrary shift effect can be well-interpreted by the charge interaction in  $\omega_+^-$  modes.

In this paper, we study the plasmon hybridization picture of Au–silica–Au multilayer nanoshells from the optical extinction spectrum and the charge density distribution. The shift of the

extinction peaks dependent on the Au core radius or the Au shell thickness is investigated by the charge interaction analysis of the plasmon resonance modes. It is shown that, with the reduction in the distance between the Au core and the Au shell, the high energy peak in the optical spectrum is converted from the  $\omega_+^+$  mode to the  $\omega_+^-$  mode; i.e., the energy reversion of the  $\omega_+^-$  mode and the  $\omega_+^+$  mode happens. Moreover, the interesting contrary shift effect of the high energy peak in the spectrum with different relative values of the dielectric constant of the middle silica and outer surrounding can be well-explained by the charge interaction in the  $\omega_+^-$  modes. Our study could offer a modified way based on the charge interaction analysis to study plasmon responses in the optical spectrum of metal nanostructures and give new insight into the plasmon hybridization theory. The approach based on the charge interaction analysis to study plasmon responses can easily be generalized to more complex metal nanostructures, such as N-layers metal–dielectric or bimetal (Au and Ag)–dielectric particles.<sup>22–30</sup>

## 2. THEORETICAL METHODS

The Au–silica–Au multilayer nanoshells we study are shown in Figure 1a. The radii of the Au core, middle silica layer, and Au shell are  $r_1$ ,  $r_2$ ,  $r_3$ . We have simulated the optical extinction spectra of the nanoshells by the three-dimensional finite-difference time domain (FDTD) method. The surface charge density of the multilayer nanoshells is calculated by taking the divergence of electric field. The multilayer nanoshell structures we studied are in the size region (diameter about 100 nm) where successful particle fabrications have been reported.<sup>4,8,15</sup> The incident radiation propagates in the +x direction, and the polarization vector of incident light is along the z axis. The dielectric properties for gold are taken from ref 31. The dielectric constant of the silica layer  $\epsilon_1$  is set as 2.04, and the dielectric constant of the embedding medium  $\epsilon_2$  is set as 1.00.

The plasmon hybridization schematic of the Au core mode  $\omega_s$  and the Au shell modes  $\omega_+^o$  and  $\omega_-^o$  is shown in Figure 1b. The dashed line in Figure 1b indicates the enhanced coupling between the Au core and the Au shell. Increasing the plasmon interaction between the Au sphere mode  $\omega_s$  and the Au shell modes  $\omega_+^o$  and  $\omega_-^o$  will cause the increase in the energy of coupling modes  $\omega_+^+$  and  $\omega_+^-$ , but the decrease in the energy of coupling modes  $\omega_-^+$  and  $\omega_-^-$ . Then the energy reversion of  $\omega_+^+$  and  $\omega_+^-$  modes may occur, as we will discuss below. The charge distributions of the coupling modes  $\omega_+^-$ ,  $\omega_+^+$ , and  $\omega_-^-$  are shown in Figure 1c.

Figure 1d–f shows the schematic of the charge interaction between the Au core and the Au shell in the  $\omega_+^-$ ,  $\omega_+^+$ , and  $\omega_-^-$  plasmon modes, respectively. In the  $\omega_+^-$  and  $\omega_+^+$  modes, the charges on the inner surface and the outer surface of the Au shell have the same signs. The charge interaction between the Au core and the Au shell has only one type of interaction (attraction in the  $\omega_+^-$  modes or repulsion in the  $\omega_+^+$  modes). On the other hand, in the  $\omega_-^-$  modes, the charges on the inner surface and the outer surface of the Au shell have the opposite signs. There are two types of interactions in the  $\omega_-^-$  modes. The charge interaction between the Au core and the inner surface of the Au shell is attractive, whereas the charge interaction between the Au core and the outer surface of Au shell is repulsive. As discussed in the following section, the two types of interactions in the  $\omega_-^-$  modes will be important to explain the contrary shift effect of the high energy extinction peaks with different dielectric constants of the middle silica

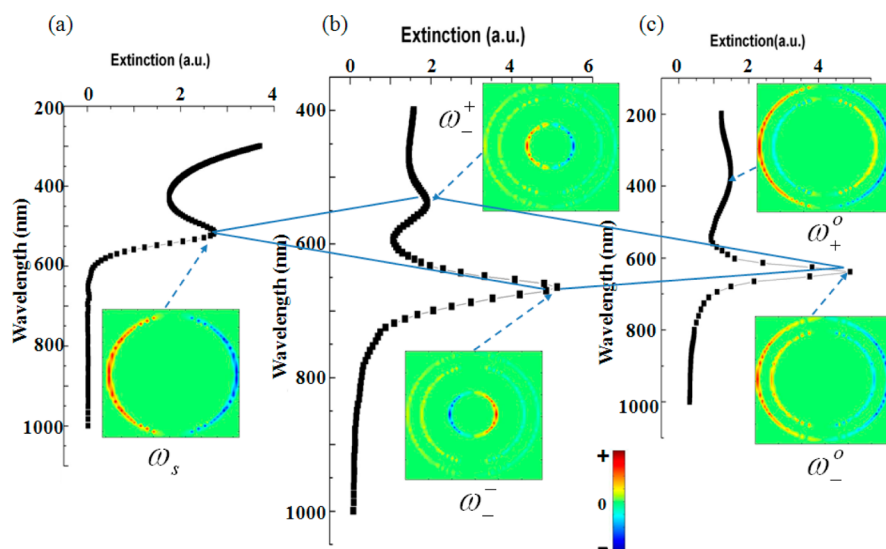


**Figure 2.** Accustomed plasmon hybridization picture of Au–silica–Au multilayer nanoshells. The extinction spectra of (a) Au sphere ( $r_1 = 20$  nm,  $\epsilon_2 = 1.00$ ), (b) Au–silica–Au multilayer nanoshells ( $[r_1, r_2, r_3] = [20, 44, 56]$  nm,  $\epsilon_1 = 2.04$ , and  $\epsilon_2 = 1.00$ ), and (c) silica–Au nanoshell ( $[r_1, r_2] = [44, 56]$  nm,  $\epsilon_1 = 2.04$ , and  $\epsilon_2 = 1.00$ ). The charge density distributions of the extinction peaks are also shown.

shell and outer surrounding. Moreover, it is noted that increasing the electrostatic repulsion between the Au core and the Au shell will enhance the energy of coupled plasmon modes, whereas increasing the electrostatic attraction between the Au core and the Au shell will reduce the energy of coupled plasmon modes. Increasing the electrostatic interaction between the Au core and the Au shell can be realized by changing the geometric parameters of nanoshells, such as increasing the Au core radius  $r_1$  at fixed  $r_2, r_3$ .

### 3. RESULTS AND DISCUSSIONS

We first give the accustomed plasmon hybridization picture<sup>5,7,8</sup> of Au–silica–Au multilayer nanoshells as shown in Figure 2. The extinction spectra of the Au sphere ( $r_1 = 20$  nm), silica–Au nanoshell ( $[r_1, r_2] = [44, 56]$  nm), and Au–silica–Au multilayer nanoshells ( $[r_1, r_2, r_3] = [20, 44, 56]$  nm) are calculated. The charge density distributions are given as the inserted pictures to characterize the corresponding resonance modes of the extinction peaks. As seen from Figure 2, the hybridization of the Au sphere mode  $|\omega_s\rangle$  (515 nm) and the Au shell bonding mode  $|\omega_-^0\rangle$  (638 nm) creates the  $|\omega_-^-\rangle$  mode (664 nm, the low energy peak) and  $|\omega_+^-\rangle$  mode (534 nm, the high energy peak) of Au–silica–Au nanoshells. The higher-energy modes coupled between the Au shell antibonding mode  $|\omega_+^0\rangle$  (361 nm) and the Au sphere mode  $|\omega_s\rangle$  (515 nm) are often unvisualized in the optical spectrum of Au–silica–Au nanoshells. Since the low energy peak in the optical spectrum of Au–silica–Au nanoshells is always the  $|\omega_-^-\rangle$  mode, in the following, we mainly consider the charge density distribution of the high energy peak in the optical spectrum.

We then consider the influence of the Au core radius ( $r_1$ ) on the extinction properties of Au–silica–Au nanoshells. Figure 3 shows the extinction spectra of Au–silica–Au multilayer nanoshells with  $r_1 = 12, 16, 20, 24, 28, 32, 36$ , and 40 nm at  $r_2 = 44$  nm,  $r_3 = 56$  nm. It is seen that the low energy extinction peaks red shift and the high energy extinction peaks blue shift with the increase in the Au core radius. The results agree with the previous study on the Au–silica–Au multilayer shell.<sup>6,7</sup> The charge density distributions of the high energy peaks of the spectrum are also shown in Figure 3. It is seen that the high

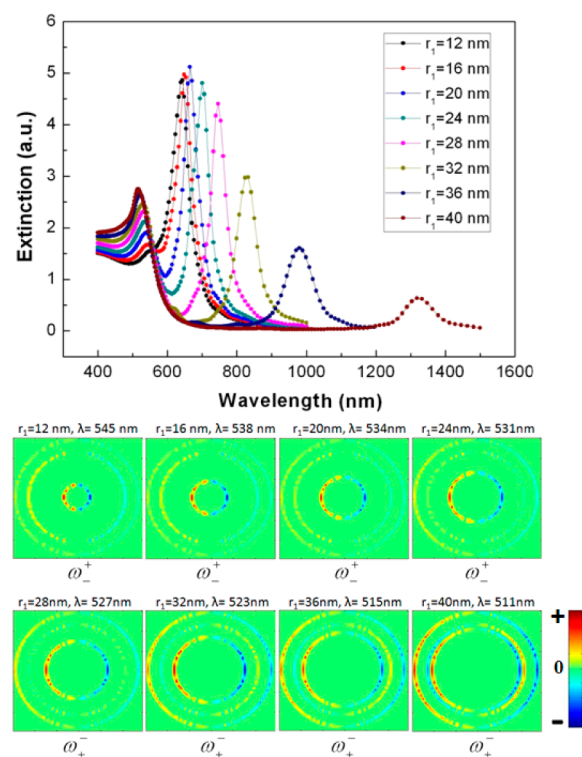


**Figure 3.** Extinction efficiency of the Au–silica–Au multilayer nanoshells with different  $r_1$  ( $r_1 = 12, 16, 20, 24, 28, 32, 36$ , and 40 nm,  $r_2 = 44$  nm,  $r_3 = 56$  nm) at  $\epsilon_1 = 2.04$  and  $\epsilon_2 = 1.00$ . The charge density distributions of the high energy peaks of the nanoshells at different  $r_1$  are shown.

energy peaks of the spectrum is in  $|\omega_+^-\rangle$  modes when the Au core is small ( $r_1 \leq 24$  nm), but the plasmon mode  $|\omega_+^-\rangle$  is converted to  $|\omega_-^-\rangle$  modes when the Au core radius is larger than 28 nm. This can be understood as follows. With the increase in the Au core radius, the electrostatic repulsion enhances between the Au core and the Au shell with charges of the same signs in the  $|\omega_+^-\rangle$  modes (as shown in Figure 1e). As the Au core is close to the inner surface of the Au shell, the energy



of the  $|\omega_+^+\rangle$  mode increases beyond the  $|\omega_+^-\rangle$  mode (as shown in Figure 1d) in which the charges on the Au core and the inner surface of the Au shell are different signs. Then the visual high energy peaks in the spectrum are converted to the  $|\omega_+^-\rangle$  modes. Here, it implies the physical origin that the extinction peaks preferentially occupy the lower-energy level of hybrid plasmon modes. From the view of the energy level analysis in plasmon hybridization theory, an increase in the inner Au core radius will decrease the intermediate silica layer thickness and increase the plasmon interaction between the Au sphere mode  $|\omega_s^0\rangle$  and the Au shell modes  $|\omega_-^0\rangle$  and  $|\omega_+^0\rangle$ . Thus, the energy of coupling modes  $|\omega_-^+\rangle$  and  $|\omega_+^+\rangle$  rises, whereas the energy of coupling modes  $|\omega_-^-\rangle$  and  $|\omega_+^-\rangle$  drops, which is shown in Figure 1b. Then the interesting reversion of  $|\omega_-^+\rangle$  and  $|\omega_+^-\rangle$  modes occurs, and the high energy peak in the optical spectrum preferentially occupies the lower-energy  $|\omega_-^+\rangle$  modes instead of  $|\omega_+^-\rangle$  modes. The similar charge distribution of  $|\omega_+^-\rangle$  modes is also reported by Ho et al. in the study on Ag–silica–Ag multilayer nanoshells.<sup>30</sup>

As shown in Figure 3, we can see that the surface charge on the inner surface of the Au shell changes from negative (positive) to positive (negative) at the right (left) side of the profile with increased  $r_1$ . It is interestingly found that the inner surface of the metal shell has nearly no surface charge at about  $r_1 = 28$  nm. In this case, a special plasmon hybridization mode (named as  $|\omega_0\rangle$ ) is generated, which has the same sign charge on the surface of the Au core and on the outer surface of the Au shell but has no charge on the inner surface of the Au shell (details are in the Supporting Information). The  $|\omega_0\rangle$  mode could be understood as the combination of the  $|\omega_-^-\rangle$  mode and the  $|\omega_+^+\rangle$  mode. From the view of the energy level analysis in plasmon hybridization theory, as  $r_1$  is increased, the energy of coupling modes  $|\omega_+^+\rangle$  rises, whereas the energy of coupling modes  $|\omega_-^-\rangle$  reduces. At a certain value of  $r_1$ , the energy of the  $|\omega_+^-\rangle$  mode and the  $|\omega_-^+\rangle$  mode may be equal, and the energy level of the  $|\omega_+^-\rangle$  mode and the energy level of the  $|\omega_-^+\rangle$  mode are combined into one energy level of the  $|\omega_0\rangle$  mode. At this time, it seems that the  $|\omega_+^-\rangle$  mode and the  $|\omega_-^+\rangle$  mode occur simultaneously in the multilayered nanoshells, and the opposite sign charge of the  $|\omega_+^-\rangle$  mode and the  $|\omega_-^+\rangle$  mode is neutralized on the inner surface of the Au shell, which leads to the generation of the  $|\omega_0\rangle$  mode.

Here, we can explain the shift of the low energy and high energy extinction peaks dependent on the Au core radius ( $r_1$ ) from the perspective of charge interaction in plasmon modes. For the low energy peaks in  $|\omega_-^-\rangle$  modes (as shown in Figure 1f), increasing the Au core radius will increase the electrostatic attraction between the Au core and the Au shell with charges of opposite signs, which leads to reduction of energy of plasmon mode  $|\omega_-^-\rangle$  accompanied by a red shift. For the high energy peaks in  $|\omega_+^+\rangle$  modes (as shown in Figure 1e), increasing the Au core radius will enhance the electrostatic repulsion between the Au core and the Au shell with charges of the same signs, which results in the enhancement of energy of  $|\omega_+^+\rangle$  modes accompanied by the blue shift of the extinction peaks. On the other hand, for the high energy peaks in  $|\omega_+^-\rangle$  modes (as shown in Figure 1d), there are different signs of charge on the inner surface and the outer surface of the Au shell, but the induced charge on the outer surface is greater than that on the inner surface due to the dielectric screening<sup>5,19</sup> of the middle silica layer. The charge on the outer surface of the Au shell will play a dominant role during the plasmon interaction between the Au core and the Au shell. Therefore, when the Au core

radius increases, the extinction peaks also blue shift in the  $|\omega_+^-\rangle$  modes due to the increased electrostatic repulsion between the Au core and the outer surface of the Au shell with charges of the same signs. The alternative case that the charge on the inner surface of the Au shell plays a dominant role in the  $|\omega_+^-\rangle$  mode will be discussed in a later section.

To further verify the idea that the approach of the Au core to the inner surface of the Au shell leads to the conversion from  $|\omega_+^-\rangle$  to  $|\omega_-^+\rangle$  modes, we reduce the distance between the Au core and the inner surface of the Au shell by increasing the thickness of the Au shell at fixed  $r_3$ . In Figure 4, we show the

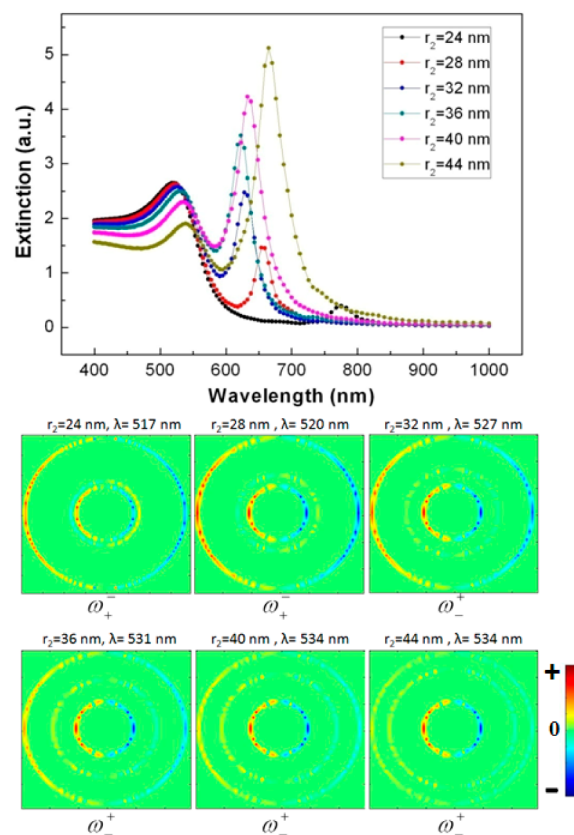


**Figure 4.** Extinction efficiency of the Au–silica–Au multilayer nanoshells with different  $r_2$  ( $r_2 = 24, 28, 32, 36, 40$ , and  $44$  nm,  $r_1 = 20$  nm,  $r_3 = 56$  nm) at  $\epsilon_1 = 2.04$  and  $\epsilon_2 = 1.00$ . The charge density distributions of the high energy peaks of the nanoshells at different  $r_2$  are shown.

extinction spectra of Au–silica–Au multilayer nanoshells with  $r_2 = 24, 28, 32, 36, 40$ , and  $44$  nm at  $r_1 = 20$  nm,  $r_3 = 56$  nm. It is seen that, with the increase in the Au shell thickness, the low energy extinction peaks first blue shift (at  $r_2 = 36, 40, 44$  nm) and then red shift (at  $r_2 = 24, 28, 32$  nm), whereas the high energy extinction peaks blue shift. From the charge distribution of the high energy peaks, we find that, during the increase of the Au shell thickness with fixed  $r_1$  and  $r_3$ , the plasmon mode  $|\omega_+^+\rangle$  is also converted to  $|\omega_+^-\rangle$  modes (when  $r_2 \leq 28$  nm) due to the increasing electrostatic repulsion while the Au core approaches to the inner surface of the Au shell, which is similar to the above discussions. The  $|\omega_0\rangle$  mode in this geometry is discussed in the Supporting Information.

The shift of the low energy and high energy extinction peaks dependent on the Au shell thickness with fixed  $r_3$  can be interpreted by the charge interaction analysis of the resonance

modes as follows. For the low energy peaks in  $|\omega_-^- \rangle$  modes, when the Au shell thickness is small ( $r_2 = 36, 40, 44$  nm), the distance between the Au core and the inner surface of the Au shell is relatively large. Then the interaction between the charge on the inner Au core and the outer Au shell is weak, and the Au shell mode  $|\omega_-^0 \rangle$  plays a major role in the contribution to the coupled  $|\omega_-^- \rangle$  modes. As well-known results, increasing the thickness of the Au nanoshell at a fixed overall size will decrease the ratio of the core size to shell thickness of the Au nanoshell, which induces a blue shift of the extinction peaks in the spectrum (increase of energy in Au shell mode  $|\omega_-^0 \rangle$ ). Thus, the energy of  $|\omega_-^- \rangle$  modes increases with the increased thickness of the Au shell when the Au shell thickness is small ( $r_2 = 36, 40, 44$  nm), which results in the blue shift of the low energy peaks. However, when the Au shell thickness is large ( $r_2 = 24, 28, 32$  nm), the distance between the Au core and the inner surface of the Au shell is relatively small. The interaction between the inner Au core and the outer Au shell is strong and plays a major role. Therefore, when the Au shell thickness is large ( $r_2 = 24, 28, 32$  nm), increasing the Au shell thickness will increase the electrostatic attraction between the inner Au core and the outer Au shell with charges of opposite signs (as shown in Figure 1f), which results in an energy reduction of the  $|\omega_-^- \rangle$  mode accompanied by the red shift. For the high energy peaks in  $|\omega_-^+ \rangle$  modes (as shown in Figure 1e), increasing the Au shell thickness with fixed  $r_3$  will enhance the electrostatic repulsion between the Au core and the Au shell with charges of the same signs, which results in the blue shift of the extinction peaks. Besides, for the high energy peaks in  $|\omega_+^- \rangle$  modes (as shown in Figure 1d), the charge induced on the outer surface of the Au shell is larger than that on the inner surface of the Au shell due to the dielectric screening as discussed above. Then the charge on the outer surface of the Au shell will play a dominant role during the plasmon interaction between the Au core and the Au shell. As the Au shell thickness increases at fixed  $r_3$ , the extinction peaks also blue shift in the  $|\omega_+^- \rangle$  modes due to the increased electrostatic repulsion between the Au core and the outer surface of the Au shell with charges of the same signs.

Furthermore, we discuss an interesting contrary shift of the high energy peak in the spectrum with the increasing of the Au core radius, which can be a proof for conversion from the  $|\omega_-^+ \rangle$  to  $|\omega_+^- \rangle$  modes we propose. In a previous work, Zhu et al.<sup>7</sup> reported that the shift of the high energy extinction peaks in the spectrum of Au–silica–Au nanoshells with the increasing Au core radius at fixed  $r_2$  and  $r_3$  depends on the relative dielectric constant of the middle silica layer ( $\epsilon_1$ ) and the embedding medium ( $\epsilon_2$ ). When the dielectric constant of the middle silica layer is higher, the high energy extinction peaks blue shift with the increasing Au core radius. Otherwise, when the dielectric constant of the embedding medium is higher, the high energy extinction peaks red shift with the increasing Au core radius. It is difficult to explain this contrary shift effect by the  $|\omega_-^+ \rangle$  modes in the plasmon hybridization theory. In the simulations of Figure 3,  $\epsilon_1$  is set to be 2.04 and  $\epsilon_2$  is set to be 1.0. The blue shift of the high energy extinction peaks with the increasing Au core radius as shown in Figure 3 is consistent with Zhu et al.'s work. We also calculate the extinction spectra of Au–silica–Au multilayer nanoshells ( $r_1 = 24, 28, 32, 36$  nm,  $r_2 = 44$  nm,  $r_3 = 56$  nm) with the increasing Au core radius at  $\epsilon_1 = 1.21$  and  $\epsilon_2 = 2.25$ . The simulated results are shown in Figure 5a. Similar to Figure 3, it is seen that low energy extinction peaks red shift with increasing of the Au core radius. The middle small extinction peaks between the high energy peaks and the low

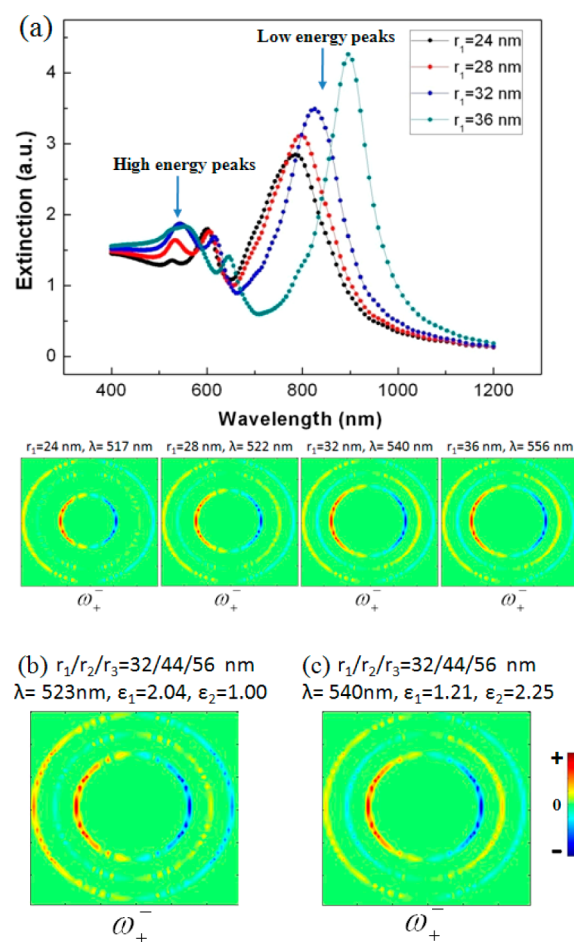


**Figure 5.** (a) Extinction efficiency of the Au–silica–Au multilayer nanoshells with different  $r_1 = 24, 28, 32$ , and  $36$  nm when  $r_2 = 44$  nm and  $r_3 = 56$  nm at  $\epsilon_1 = 1.21$  and  $\epsilon_2 = 2.25$ . The charge density distributions of the high energy peaks of the nanoshells at different  $r_1$  are shown. (b, c) The charge density distributions of the high energy peaks of Au–silica–Au multilayer nanoshells ( $[r_1, r_2, r_3] = 32, 44, 56$  nm) at  $\epsilon_1 = 2.04$  and  $\epsilon_2 = 1.00$  (b) and  $\epsilon_1 = 1.21$  and  $\epsilon_2 = 2.25$  (c).

energy peaks are the extinction peaks induced by the retardation effect.<sup>32</sup> Consistent with Zhu et al.'s work, the high energy peaks red shift with the increasing of the Au core radius as shown in Figure 5a. The charge distribution of the high energy peaks is shown as  $|\omega_+^- \rangle$  modes in Figure 5a.

The contrary shift of the high energy peaks dependent on the  $\epsilon_1$  and  $\epsilon_2$  can be well-explained by the charge interaction in  $|\omega_+^- \rangle$  modes (as shown in Figure 1d) as follows: when  $\epsilon_1$  is larger than  $\epsilon_2$ , the induced charge on the outer surface is greater than that on the inner surface of the Au shell due to the dielectric screening; then the charge on the outer surface of the Au shell will play a dominant role during the plasmon interaction between the Au core and the Au shell in the  $|\omega_+^- \rangle$  modes. Thus, the high energy extinction peaks blue shift with the increasing Au core radius due to the increased electrostatic repulsion between the Au core and the outer surface of the Au shell with charges of the same signs. On the other hand, when  $\epsilon_2$  is larger than  $\epsilon_1$ , the induced charge on the inner surface is greater than that on the outer surface of the Au shell. Then the charge on the inner surface of the Au shell will play a dominant role during the plasmon interaction between the Au core and the Au shell in the  $|\omega_+^- \rangle$  modes. Thus, the high energy extinction peaks red shift with the increasing Au core radius due

to the increased electrostatic attraction between the Au core and the inner surface of Au shell with charges of different signs. The induced charge density distribution of the high energy extinction peaks of the Au–silica–Au multilayer nanoshells with the same size at different relative dielectric constants of the middle silica layer and the embedding medium is shown in Figure 5b,c. As shown in Figure 5b,c, the different charge density distribution on the inner surface and outer surface of the Au shell is qualitatively demonstrated.

#### 4. CONCLUSIONS

In this work, we study the charge density distribution of the plasmon resonant modes of the Au–silica–Au multilayer nanoshells by FDTD simulations. We find that the high energy extinction peak of the optical spectrum is converted from  $\omega_+^-$  modes to  $\omega_+^+$  modes when the Au core is close to the inner surface of the Au shell. It is due to the energy reversion of  $\omega_+^-$  and  $\omega_+^+$  plasmon modes induced by the increasing plasmon interaction between the Au core and the Au shell. The shift of the extinction peaks dependent on the Au core radius or the Au shell thickness is interpreted by the charge interaction analysis of the plasmon modes. Furthermore, we explain the contrary shift effect of the high energy peak in the spectrum at different relative values of the dielectric constant of the middle silica shell and outer surrounding by the charge interaction in the  $\omega_+^-$  modes. Our study shows that the charge interaction analysis of the resonant plasmon mode is a necessary supplement to the plasmon hybridization theory for studying the plasmon responses of the metal nanostructures.

#### ■ ASSOCIATED CONTENT

##### Supporting Information

The extinction spectra and the charge density distributions of the plasmon hybridization mode  $\omega_0$ . This material is available free of charge via the Internet at <http://pubs.acs.org>.

#### ■ AUTHOR INFORMATION

##### Corresponding Author

\*E-mail: [qiansun@nankai.edu.cn](mailto:qiansun@nankai.edu.cn). Phone: 86-022-23506238. Fax: 86-022-23506238.

##### Notes

The authors declare no competing financial interest.

#### ■ ACKNOWLEDGMENTS

This work is supported by National Natural Science Foundation of China (11304164, 61178004), the Specialized Research Fund for the Doctoral Program of Higher Education of China (20130031120006, 20110031120005), the Tianjin Natural Science Foundation (13JCQNJC01700), and the Program for Changjiang Scholars and Innovative Research Team in Nankai University.

#### ■ REFERENCES

- (1) Hirsch, L. R.; Stafford, R. J.; Bankson, J. A.; Sershen, S. R.; Rivera, B.; Price, R. E.; Hazle, J. D.; Halas, N. J.; West, J. L. Nanoshell-Mediated Near-Infrared Thermal Therapy of Tumors under Magnetic Resonance Guidance. *Proc. Natl. Acad. Sci. U.S.A.* **2003**, *100*, 13549–13554.
- (2) Gobin, A. M.; Lee, M. H.; Halas, N. J.; James, W. D.; Drezek, R. A.; West, J. L. Near-Infrared Resonant Nanoshells for Combined Optical Imaging and Photothermal Cancer Therapy. *Nano Lett.* **2007**, *7*, 1929–1934.

- (3) Choi, M. R.; Stanton-Maxey, K. J.; Stanley, J. K.; Levin, C. S.; Bardhan, R.; Akin, D.; Badve, S.; Sturgis, J.; Robinson, J. P.; Bashir, R.; et al. A Cellular Trojan Horse for Delivery of Therapeutic Nanoparticles into Tumors. *Nano Lett.* **2007**, *7*, 3759–3765.
- (4) Xia, X. H.; Liu, Y.; Backman, V.; Ameer, G. A. Engineering Sub-100 nm Multi-layer Nanoshells. *Nanotechnology* **2006**, *17*, S435–S440.
- (5) Wu, D. J.; Liu, X. Tunable Near-Infrared Optical Properties of Three-Layered Gold–Silica–Gold Nanoparticles. *Appl. Phys. B: Lasers Opt.* **2009**, *97*, 193–197.
- (6) Hu, Y.; Fleming, R. C.; Drezek, R. A. Optical Properties of Gold–Silica–Gold Multilayer Nanoshells. *Opt. Express* **2008**, *16*, 19579–19591.
- (7) Zhu, J.; Li, J. J.; Zhao, J. W. Tuning the Dipolar Plasmon Hybridization of Multishell Metal–Dielectric Nanostructure: Gold Nanosphere in a Gold Nanoshell. *Plasmonics* **2011**, *6*, 527–534.
- (8) Bardhan, R.; Mukherjee, S.; Mirin, N. A.; Levit, S. D.; Nordlander, P.; Halas, N. J. Nanosphere-in-a-Nanoshell: A Simple Nanomaterial. *J. Phys. Chem. C* **2010**, *114*, 7378–7383.
- (9) Zhu, J.; Li, J. J.; Zhao, J. W. Frequency-Dependent Polarization Properties of Local Electric Field in Gold–Dielectric Multi-Nanoshells. *Plasmonics* **2013**, *8*, 417–424.
- (10) Liu, C. H.; Mi, C. C.; Li, B. Q. The Plasmon Resonance of a Multilayered Gold Nanoshell and its Potential Bioapplications. *IEEE Trans. Nanotechnol.* **2011**, *10*, 797–805.
- (11) Wu, D. J.; Jiang, S. M.; Cheng, Y.; Liu, X. J. Modulation of Anisotropic Middle Layer on the Plasmon Couplings in Sandwiched Gold Nanoshells. *Gold Bull.* **2012**, *45*, 197–201.
- (12) Zhu, J.; Ren, Y. J.; Zhao, S. M.; Zhao, J. W. The Effect of Inserted Gold Nanosphere on the Local Field Enhancement of Gold Nanoshell. *Mater. Chem. Phys.* **2012**, *133*, 1060–1065.
- (13) Bahari, A.; Moghadam, F. R. Third Order Harmonics Generation in Multilayer Nanoshells. *Opt. Commun.* **2012**, *285*, 3295–3299.
- (14) Peña-Rodríguez, O.; Rivera, A.; Campoy-Quiles, M.; Pal, U. Tunable Fano Resonance in Symmetric Multilayered Gold Nanoshells. *Nanoscale* **2013**, *5*, 209–216.
- (15) Mukherjee, S.; Sobhani, H.; Lassiter, J. B.; Bardhan, R.; Nordlander, P.; Halas, N. J. Nanoshells: Nanoparticles with Built-in Fano Resonances. *Nano Lett.* **2010**, *10*, 2694–2701.
- (16) Hu, Y.; Noelck, S. J.; Drezek, R. A. Symmetry Breaking in Gold–Silica–Gold Multilayer Nanoshells. *ACS Nano* **2010**, *4*, 1521–1528.
- (17) Wang, M.; Cao, M.; Chen, X.; Gu, N. Subradiant Plasmon Modes in Multilayer Metal–Dielectric Nanoshells. *J. Phys. Chem. C* **2011**, *115*, 20920–20925.
- (18) Prodan, E.; Radloff, C.; Halas, N. J.; Nordlander, P. Hybridization Model for the Plasmon Response of Complex Nanostructures. *Science* **2003**, *302*, 419–422.
- (19) Prodan, E.; Nordlander, P. Plasmon Hybridization in Spherical Nanoparticles. *J. Chem. Phys.* **2004**, *120*, 5444–5454.
- (20) Park, T.; Nordlander, P. On the Nature of the Bonding and Antibonding Metallic Film and Nanoshell Plasmons. *Chem. Phys. Lett.* **2009**, *427*, 228–231.
- (21) Zhu, J.; Li, J. J.; Yuan, L.; Zhao, J. W. Optimization of Three-Layered Au–Ag Bimetallic Nanoshells for Triple-Bands Surface Plasmon Resonance. *J. Phys. Chem. C* **2012**, *116*, 11734–11740.
- (22) Peña-Rodríguez, O.; Pal, U. Geometrical Tunability of Linear Optical Response of Silica–Gold Double Concentric Nanoshells. *J. Phys. Chem. C* **2010**, *114*, 4414–4417.
- (23) K. Kodali, A.; Schulmerich, M. V.; Palekar, R.; Llorca, X.; Bhargava, R. Optimized Nanospherical Layered Alternating Metal–Dielectric Probes for Optical Sensing. *Opt. Express* **2010**, *18*, 23302–23313.
- (24) K. Kodali, A.; Llorca, X.; Bhargava, R. Optimally Designed Nanolayered Metal–Dielectric Particles as Probes for Massively Multiplexed and Ultrasensitive Molecular Assays. *Proc. Natl. Acad. Sci. U.S.A.* **2010**, *107*, 13620–13625.



- (25) Khosravi, H.; Daneshfar, N.; Bahari, A. Theoretical Study of the Light Scattering From Two Alternating Concentric Double Silica-Gold Nanoshell. *Phys. Plasmas* **2010**, *17*, 053302.
- (26) Liu, C. H.; Li, B. Q. Computational Multiscattering of Spherical Multilayered Gold Nanoshells. *J. Phys. Chem. C* **2011**, *115*, 5323–5333.
- (27) Wu, D. J.; Jiang, S. M.; Liu, X. J. Tunable Fano Resonances in Three-Layered Bimetallic Au and Ag Nanoshell. *J. Phys. Chem. C* **2011**, *115*, 23797–23801.
- (28) Peña-Rodríguez, O.; Pal, U. Enhanced Plasmonic Behavior of Bimetallic (Ag-Au) Multilayered Spheres. *Nanoscale Res. Lett.* **2011**, *6*, 279.
- (29) Shirzaditabar, F.; Saliminasab, M. Geometrical Parameters Effects on Local Electric Field Enhancement of Silver-Dielectric-Silver Multilayer Nanoshell. *Phys. Plasmas* **2013**, *20*, 052109.
- (30) Ho, J. F.; Luk'yanchuk, B.; Zhang, J. B. Tunable Fano Resonances in Silver–Silica–Silver Multilayer Nanoshells. *Appl. Phys. A: Mater. Sci. Process.* **2012**, *107*, 133–137.
- (31) Johnson, P. B.; Christy, R. W. Optical Constants of the Noble Metals. *Phys. Rev. B: Condens. Matter* **1972**, *6*, 4370–4379.
- (32) Turner, M. D.; Hossain, M. M.; Gu, M. The Effects of Retardation on Plasmon Hybridization Within Metallic Nanostructures. *New J. Phys.* **2010**, *12*, 083062.